JOURNAL OF GUIDANCE, CONTROL, AND DYNAMICS
Vol. 21, No. 6, November–December 1998

Time-Optimal Turn to a Heading: An Improved Analytic Solution

Werner Grimm* and Markus Hans†
University of Stuttgart, Stuttgart D-70550, Germany

Aircraft turning performance in the horizontal plane is addressed. The task is to reach a specified heading and speed in minimum time. The objective is to obtain a closed-form feedback expression for the optimal turn rate in the case in which load-factor constraints do not become active. The starting point is the boundary-value problem derived from the necessary conditions of optimal control. An analytic solution results for constant maximum thrust and a parabolic drag polar with constant coefficients. The extension to previous results is twofold: First, the solution is determined for all boundary conditions in the flight envelope. In many cases a composite structure made up of two different control types occurs. Second, the dynamic model includes the drag induced by the vertical lift component, which was neglected in previous work. The feedback expression for the optimal turn rate is utilized to guide an aircraft with realistic dynamics. The desired terminal conditions are reached accurately as long as load-factor constraints do not become active. The agreement of simulated flight paths using this guidance law and optimal turns obtained from open-loop trajectory optimization depends on the particular boundary conditions.

Nomenclature

c_{D0} = zero-lift drag coefficient
c_L = lift coefficient
D = drag
g = gravitational acceleration
k = factor in the drag polar
M = Mach number
m = aircraft mass
q = dynamic pressure
S = reference wing area
T = thrust
u = turn rate $\dot{\chi}$
u_s = steady-state turn rate
V = speed
W = weight, $m \times g$
μ = bank angle
ρ = air density
χ = heading angle

I. Introduction

AIRCRAFT turns in the horizontal plane have been a favorite subject in trajectory optimization since the early seventies,[1] and it is beyond the scope of this introduction to discuss all of the work done. Although the subject sounds simple, optimal turns can have a complicated structure because of the bounded lift. There may be boosting, coasting, and sustaining arcs flown with maximum or interior load factor. Vinh[2] gives an overview of the possible switching structures with respect to thrust control.

In general, the optimal turn is the solution of a multipoint boundary-value problem (MPBVP). Because of the availability of efficient multiple shooting algorithms,[3,4] the offline numerical computation has become almost routine work, whereas near-optimal real-time control is still an open research area. Neighboring optimal feedback control[5] directly uses the output of the multiple shooting algorithm. Linearization of the necessary conditions of optimality leads to a near-optimal feedback control in the neighborhood of the nominal trajectory. General state and control constraints can be included in the concept.[6]

The artificial introduction of multiple timescales in the framework of singular perturbations yields a global feedback law valid throughout the whole state space. Simultaneously, the turning maneuver can be embedded into a more general differential game formulation. Shinar[7,8] suggests deriving the reduced solution from the kinematics only and treating the speed and heading dynamics as first and second boundary layer, respectively. Another timescale definition leads to the energy-state model, which allows analysis of three-dimensional turns.[9–11] Because altitude is considered to be a pseudocontrol, the remaining state dynamics are similar to motion in the horizontal plane. A typical property of energy-state extremals is that they perform most of the turning on the corner velocity locus. A feedback control based on energy-state solutions needs a set of extremals that covers the whole state space.[12]

Analytic solution here means obtaining the optimal control as a function of the state variables in closed form. At most, there may be a few parameters that are determined numerically from some nonlinear equations. The advantage for real-time operation would be that no precomputed trajectories are required. If the dynamics are not divided into timescales, other simplifications about the design model are necessary to arrive at a closed-form solution. If the terminal conditions depend on the position coordinates, speed typically is regarded as a constant.[1,13,14] Under this assumption, optimal trajectories consist of straight-line segments and circular subarcs flown at maximum bank angle. Only a penalty on the control effort in the performance index leads to noncircular paths.[15] Shapira and Ben-Asher[16] suggest a variable speed model, which maintains the access to a closed-form solution. Speed is modeled as a linearly decreasing function of the absolute value of the turn rate. Unlike constant-velocity extremals, the speed performs a jump at a junction of a circular arc and a straight-line segment.

If the terminal position is free, a simplified speed dynamics model can be included in the analytic approach. This simplified model has constant maximum thrust and a parabolic drag polar with constant coefficients. Under these assumptions, Vinh[2] obtains analytic solutions for the coasting and the sustaining subarc of the optimal turn to a heading. Walden[17] began analyzing turns with maximum thrust and unbounded control and presented first results for small values of the commanded heading change. Motivated by the work of Walden,[17] the present analysis answers the question about large turn angles and finds the solution for any set of boundary conditions within the flight envelope. Because control constraints are not included, the results are applicable only if the turn-rate command does not exceed the load-factor limit or the maximum lift coefficient.

The optimal turn rate is computed with two different dynamic models. The first one, which also is used by Walden[17], neglects the drag induced by the vertical lift component, whereas the second one

Received Nov. 24, 1997; revision received April 13, 1998; accepted for publication April 30, 1998.

*Research Scientist, Institute of Flight Mechanics and Control, Pfaffenwaldring 7a.
†Graduate Student, Institute of Flight Mechanics and Control, Pfaffenwaldring 7a.

does not. The scheme to derive the control law is the same as in the analytic studies referenced above. First, the state and costate equations of the MPBVP are solved up to some constants of integration. The remaining unknowns are determined from the boundary conditions, which is rarely possible in closed form. The present paper proves the existence and uniqueness of the solution in these cases and gives lower and upper bounds to facilitate a numerical solution. The paper ends with an experiment in which the optimal analytic feedback control is used to guide an aircraft with realistic dynamics and performance limits.

II. Equations of Motion

A. Flight in the Horizontal Plane

Flight in the horizontal plane is described by the differential equations

$$m\dot{V} = T - D, \qquad \dot{\chi} = (g/V)\cdot\tan\mu$$

The drag is modeled with the usual parabolic polar

$$D = q\cdot S\cdot\left(c_{D0} + k\cdot c_L^2\right)$$

where $q = \rho\cdot V^2/2$ denotes dynamic pressure. Horizontal flight requires the lift coefficient to be

$$c_L = \frac{W}{q\cdot S\cdot\cos\mu}$$

Hence, drag takes the form

$$D = q\cdot S\cdot c_{D0} + [(k\cdot W^2)/(q\cdot S)]\cdot(1+\tan^2\mu) \tag{1}$$

Introducing the turn rate $\dot{\chi} = u$ as the control facilitates the forthcoming calculations. Written with u the drag takes the form

$$D = q\cdot S\cdot c_{D0} + \frac{k\cdot W^2}{q\cdot S} + \frac{2\cdot k\cdot m^2}{\rho\cdot S}\cdot u^2$$

The following model assumptions allow for an analytic solution of the optimal control:

1) The coefficients c_{D0} and k are constants.

2) The weight is constant.

3) Thrust is at its maximum level and does not depend on V. Thus, T is a constant in the calculations later.

4) The control u is an unbounded control.

The short flight time of the considered turns permits mass flow to be neglected. For the same reason the variation of T, c_{D0}, and k during a turn should be small, which needs to be verified in simulations. The optimality of maximum thrust for unbounded control is proven below. Therefore, no extra thrust control is introduced. Item 4 means that the present analysis only considers a partial aspect of the turning problem. The results are valid only if the optimal turn-rate command does not violate the structural limit or the load limit.

Using abbreviations for constant terms the equations of motion appear in the form

$$\dot{V} = f_0(V) - C\cdot u^2, \qquad \dot{\chi} = u \tag{2}$$

with

$$f_0(V) = a_0 - a_1\cdot V^2 - \left(a_2/V^2\right) \tag{3}$$

$$a_0 = \frac{T}{m}, \qquad a_1 = \frac{\rho\cdot S\cdot c_{D0}}{2\cdot m}$$
$$a_2 = \frac{2\cdot k\cdot W^2}{m\cdot\rho\cdot S}, \qquad C = \frac{2\cdot k\cdot m}{\rho\cdot S} \tag{3a}$$

In the sequel the stationary turn rate u_s plays an important role:

$$u_s(V) = \sqrt{\frac{f_0(V)}{C}} \tag{4}$$

The existence of u_s requires f_0 to be nonnegative. In terms of flight mechanics this means that the aircraft is inside the flight envelope.

Throttle control is not introduced as an extra control. The question of whether partial thrust can improve the performance is discussed later.

B. Two Different Models

Two different models are used to analyze optimal turning in the horizontal plane.

1) *Model 1.* In this model the a_2 term in Eq. (3) is neglected. From the view of flight mechanics, this means to neglect the drag induced by the vertical lift component which compensates for the weight. For u_s [Eq. (4)] to exist, the speed must not exceed a certain upper bound:

$$V < V_u = \sqrt{a_0/a_1}$$

Model 1 was suggested by Walden[17] and is revisited to indicate to what degree the present paper contains the results of Ref. 17. Model 1 implies that stationary turning is possible for arbitrarily low speeds, which is certainly unrealistic.

2) *Model 2.* This model denotes the complete model as given in Eq. (3). V_1 and V_2 denote the boundaries of the flight envelope at the desired altitude: $f_0(V) \geq 0$ for $V_1 \leq V \leq V_2$. The minimum drag speed

$$V_m = \sqrt[4]{a_2/a_1} \tag{5}$$

which marks the peak of f_0, plays an important role later.

The f_0 histories of models 1 and 2 are depicted in Fig. 1. The coefficients a_i according to Eq. (3a) are evaluated with an F-15 model at $h = 13{,}571$ m and $V = 570$ m/s (see also case C in Sec. VI).

III. Problem Statement and Necessary Conditions

A. Optimal Control Problem

The aircraft is to perform a specified heading change in minimum time subject to given boundary values upon the speed

$$t_f \to \text{Min.}$$

subject to

$$\chi(0) = 0, \qquad \chi(t_f) = \Delta\chi, \qquad V(0) = V_0, \qquad V(t_f) = V_f$$

Without loss of generality for a symmetric aircraft, the investgation is confined to right turns: $0 < \Delta\chi \leq \pi$. For $\Delta\chi > \pi$, a left turn is the better alternative. The boundary values of the speed must lie within the flight envelope of the respective model, i.e.,

$$V_0, V_f < V_u \quad \text{for model 1}$$

and

$$V_1 < V_0, V_f < V_2 \quad \text{for model 2}$$

B. General Necessary Conditions

The existence of optimal control is assumed and the necessary conditions summarized in Ref. 18 are applied. First, the Hamiltonian is a constant:

$$H = \lambda_v\cdot\left[f_0(V) - Cu^2\right] + \lambda_\chi\cdot u \equiv -1 \tag{6}$$

The adjoint differential equations are

$$\dot{\lambda}_v = -f_0'(V)\cdot\lambda_v \tag{7}$$

$$\dot{\lambda}_\chi = 0 \tag{8}$$

The condition $0 = H_u$ determines the optimal control. In terms of state and costate variables, the optimal turn rate is given by

$$u = \lambda_\chi/2C\lambda_v \tag{9}$$

The Legendre–Clebsch condition turns out to be a sign condition for λ_v:

$$0 \leq H_{uu} = -2C\lambda_v \Rightarrow \lambda_v \leq 0 \tag{10}$$

Theorem 1: Along an optimal trajectory, there holds $\lambda_v < 0$, and λ_χ is a negative constant.

Proof: Assume that $\lambda_v = 0$ at some t. At this point the necessary conditions $H = -1$ and $0 = H_u$ would imply $\lambda_\chi\cdot u = -1$ and $\lambda_\chi = 0$. From this contradiction, one concludes that $\lambda_v \neq 0$ for all t. Together with condition (10), one obtains $\lambda_v < 0$ for all t.

Because $0 = H_u$ has the unique solution (9), $\dot{\chi} = u$ is a continuous function of time. Because of $\chi(t_f) > \chi(0)$, there must be some time $t_1 \in [0, t_f]$ with

$$\dot{\chi}(t_1) = u(t_1) = \frac{\lambda_\chi(t_1)}{2C\lambda_v(t_1)} > 0 \text{ (mean value theorem)}$$

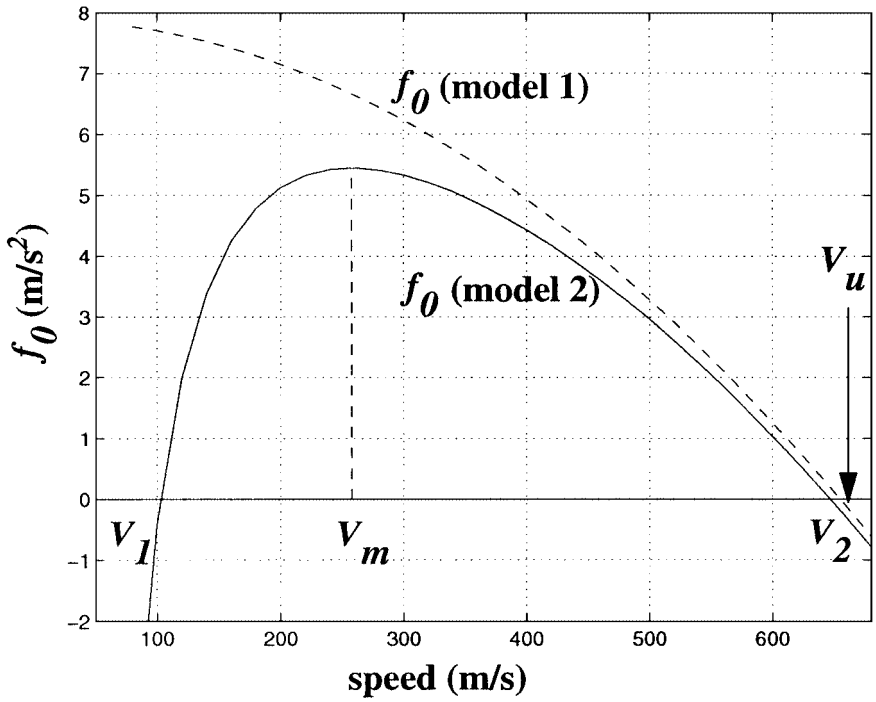

Fig. 1 Longitudinal acceleration for zero turn rate, models 1 and 2.

where $\lambda_v(t_1) < 0$ implies $\lambda_\chi(t_1) < 0$. Because λ_χ is a constant [Eq. (8)], the latter relation holds for all t. □

An immediate conclusion from $\lambda_v < 0$ is that maximum thrust is always optimal. Again it should be emphasized that this is a consequence of the assumption of unbounded control. This is no longer true if the problem formulation includes control constraints.

C. Optimal Control in Feedback Form

Eliminating λ_v from Eq. (6) yields the optimal control in the form

$$u_\pm = u^* \pm \sqrt{(u^*)^2 - [u_s(V)]^2} \tag{11}$$

with

$$u^* = -(1/\lambda_\chi) > 0$$

The sign of u^* is a consequence of Theorem 1. Hence, the optimal control is given in feedback form up to the unknown constant u^*. The crucial condition for $u_\pm$ to exist is that

$$u^* \geq u_s(V) \tag{12}$$

for all speeds occurring along the optimal trajectory.

The two optimal strategies labeled with the plus-or-minus sign differ in the resulting acceleration. Inserting $u_\pm$ into the longitudinal acceleration (2) yields

$$\dot{V}_\pm = \mp 2 \cdot C \cdot u_\pm \cdot \sqrt{(u^*)^2 - [u_s(V)]^2} \tag{13}$$

Note that u_+ is a decelerating control and u_- is an accelerating control.

D. Switching Condition

This section deals with a transition point from u_+ to u_- or vice versa at the switching speed V_s. The following theorem summarizes the result of this section.

Theorem 2: A transition from u_+ to u_- can only occur if $f_0'(V_s) < 0$. A transition from u_- to u_+ can occur only if $f_0'(V_s) > 0$.

Proof: Assume that there is a transition from u_+ to u_-. The regularity of the Hamiltonian (6) implies continuity of the control at V_s:

$$u_+(V_s) = u_-(V_s) = u_s(V_s) = u^* \tag{14}$$

Because of principle (12), one concludes that

$$u_s(V_s) = \max\{u_s(V(t)) \,|\, 0 \leq t \leq t_f\}$$

or, written with f_0,

$$f_0(V_s) = \max\{f_0(V(t)) \,|\, 0 \leq t \leq t_f\} \tag{15}$$

Because u_+ is a decelerating control and u_- is an accelerating control, V_s represents a speed minimum. This is equivalent to the f_0 maximum required by Eq. (15) only if $f_0'(V_s) < 0$. Using the same arguments, a transition from u_- to u_+ implies that $f_0'(V_s) > 0$. □

Remark: Theorem 2 yields preliminary results concerning models 1 and 2 (Sec. II.B). In model 1, f_0 is a monotonically decreasing function. Consequently, only a transition from u_+ to u_- is possible. In model 2, this transition can occur only for $V_s \geq V_m$, whereas in the subinterval $V_s \leq V_m$ a transition from u_- to u_+ can happen, which would never appear in model 1. This consideration already indicates that the results with the two models are substantially different.

E. Equation for u^*

The unknown parameter u^* is determined by the boundary conditions. Imagine that the solution is made up of only one phase, i.e., only one of the control types u_+ or u_- occurs. Then, one can write

$$\Delta\chi = \int_0^{t_f} \dot{\chi}\, \mathrm{d}t = \int_{V_0}^{V_f} \frac{u}{\dot{V}}\, \mathrm{d}V = F(u^*) \tag{16}$$

and the first step is to find a closed-form solution for F. Substitution of the independent variables is possible because, for a pure u_+ or u_- control, speed is a monotonic function of time. Equation (16) determines u^*. According to Eq. (13), the integrand in Eq. (16) is

$$\mp \frac{1}{2C\sqrt{(u^*)^2 - [u_s(V)]^2}}$$

where the different signs belong to u_+ and u_-, respectively. Clearly, the decelerating control u_+ requires $V_0 > V_f$ and vice versa for u_-. The definitions

$$V_{\min} = \min\{V_0, V_f\}, \qquad V_{\max} = \max\{V_0, V_f\}$$

allow for a unified representation of both cases:

$$F(u^*) = \int_{V_{\min}}^{V_{\max}} \frac{\mathrm{d}V}{2C\sqrt{(u^*)^2 - [u_s(V)]^2}} \tag{17}$$

Because the integrand is a decreasing function of u^* the same holds for the integral $F(u^*)$:

$$F(u^*) \text{ is decreasing in } u^* \tag{18}$$

This is an important observation for the existence and uniqueness of u^*.

Now assume that the optimal control is a sequence $u_+ - u_-$ or the other way round. Then, the integral in Eq. (16) must be split up:

$$\Delta\chi = \int_{V_0}^{V_s} \frac{u}{\dot{V}}\,\mathrm{d}V + \int_{V_s}^{V_f} \frac{u}{\dot{V}}\,\mathrm{d}V \tag{19}$$

Note that the monotonicity statement (18) is not valid in this case because the switching speed V_s depends on u^*, too.

IV. Solution for Model 1

A. Single-Phase Extremals

Single phase means that only one of the control types u_+, u_- occurs. For model 1, the integral (17) has the closed-form solution

$$F_1(u^*) = \frac{1}{2C\sqrt{C_1}} \cdot \ln \frac{\sqrt{u^{*2} - u_s^2(V_{\max})} + \sqrt{C_1}\cdot V_{\max}}{\sqrt{u^{*2} - u_s^2(V_{\min})} + \sqrt{C_1}\cdot V_{\min}} \tag{20}$$

with $C_1 = a_1/C$. The subscript 1 at the F symbol indicates the model version. Because u_s decreases for increasing speed in model 1, $u_s(V_{\min})$ is the maximum turn rate occurring along the trajectory. This fact and principle (12) determine the definition set of u^*

$$u^* \geq u_s(V_{\min}) > u_s(V_{\max})$$

As stated in Eq. (18), F is decreasing in u^*. Therefore, F takes its maximum value at the lower bound of the definition set. Consequently, there is a unique solution for u^* if $\Delta\chi \leq F_1(u_s(V_{\min}))$. Up to this point, the minimum-time turn solution is as reported by Walden.[17]

B. Two-Phase Extremals

According to Theorem 2, the sequence $u_+ - u_-$ is the only composite structure that can occur for model 1. The switching speed

$$V_s = \sqrt{\frac{a_0 - C\cdot u^{*2}}{a_1}} = \sqrt{\frac{u_s(0)^2 - u^{*2}}{C_1}}$$

obtained from Eq. (14) marks the speed minimum during the turn. Note that $u_s(0) = \sqrt{(a_0/C)}$ is an upper bound for the stationary turn rate in model 1. Equation (19) for u^* takes the form

$$\Delta\chi = \int_{V_0}^{V_s} \frac{u_+}{\dot{V}_+}\,\mathrm{d}V + \int_{V_s}^{V_f} \frac{u_-}{\dot{V}_-}\,\mathrm{d}V = G_1(u^*) \tag{21}$$

The closed-form solution (20) applies to both integrals. Using the fact that $u^* = u_s(V_s)$, the following formula results:

$$G_1(u^*) = \frac{1}{2C\sqrt{C_1}} \cdot \ln \frac{\left[\sqrt{u^{*2} - u_s^2(V_{\min})} + \sqrt{C_1}\cdot V_{\min}\right]\cdot\left[\sqrt{u^{*2} - u_s^2(V_{\max})} + \sqrt{C_1}\cdot V_{\max}\right]}{u_s^2(0) - u^{*2}}$$

The definition set of G_1 is $u_s(V_{\min}) \leq u^* < u_s(0)$, where G_1 tends to infinity on approaching the upper bound. So, the value set of G_1 is at least $[G_1(u_s(V_{\min})), \infty)$, and Eq. (21) has a solution u^* if $\Delta\chi$ is an element of the latter interval. Moreover, G_1 is an increasing function of u^*, which implies uniqueness of the solution. Summarizing all of that, one obtains the following result: The equation $\Delta\chi = G_1(u^*)$ has a unique solution u^* for $G_1(u_s(V_{\min})) \leq \Delta\chi < \infty$.

Because $G_1(u_s(V_{\min})) = F_1(u_s(V_{\min}))$, the turning problem is solved for all $\Delta\chi > 0$. The result is summarized in the following theorem.

Theorem 3: For $\Delta\chi < F_1(u_s(V_{\min}))$ the minimum-time turn is controlled exclusively by u_+ or u_-; u_+ applies to the case $V_0 > V_f$ and vice versa. For $\Delta\chi \geq F_1(u_s(V_{\min}))$, the optimal control sequence is $u_+ - u_-$.

Remark: In the special case $V_0 = V_f \Leftrightarrow V_{\min} = V_{\max}$, only two-phase solutions occur because $F_1 = 0$.

V. Solution for Model 2

A. Single-Phase Extremals

Again we are looking for a closed-form solution of the integral (17). Equation (17) takes the form

$$\frac{1}{2\sqrt{C}} \cdot \int_{V_{\min}}^{V_{\max}} \frac{V\,\mathrm{d}V}{\sqrt{a_1\cdot V^4 + \left(Cu^{*2} - a_0\right)\cdot V^2 + a_2}} = \Delta\chi$$

The substitution $y = V^2$ and the definition of appropriate constants e_0, e_1 transforms the previous equation into

$$\frac{1}{4C\sqrt{C_1}} \cdot \int_{y_{\min}}^{y_{\max}} \frac{\mathrm{d}y}{\sqrt{(y+e_0)^2 + e_1}} = \Delta\chi$$

with C_1 as in Eq. (20). The integral now can be solved in closed form. The definition

$$z = \frac{u^{*2} - u_s^2(V_m)}{2C_1} \tag{22}$$

with V_m being the minimum drag speed according to Eq. (5), abbreviates the final result. Then, z (or u^*, respectively) is determined by the equation

$$\Delta\chi = \frac{1}{4C\sqrt{C_1}} \times \ln \frac{V_{\max}^2 - V_m^2 + z + \sqrt{\left(V_{\max}^2 - V_m^2\right)^2 + 2V_{\max}^2 z}}{V_{\min}^2 - V_m^2 + z + \sqrt{\left(V_{\min}^2 - V_m^2\right)^2 + 2V_{\min}^2 z}} = F_2(u^*) \tag{23}$$

Three cases are discussed:

1) $V_{\min} \leq V_m \leq V_{\max}$: The minimum drag speed V_m being passed on the turning maneuver yields the largest turn rate u_s. Because of principle (12), the definition set of Eq. (23) is $u^* \geq u_s(V_m)$ equivalent to $z \geq 0$. The limits of F_2 for $z \to 0$ and $z \to \infty$ are ∞ and 0, and the value set of F_2 consists of all positive numbers. This guarantees the existence of u^* satisfying Eq. (23). Together with the monotonicity property (18), we get uniqueness, too: There is a unique solution u^* for any commanded turn angle $\Delta\chi$.

2) $V_m < V_{\min} \leq V_{\max}$: Now, u_s takes its maximum at $V_{\min}$. Following Eq. (12), admissible values for u^* are given by $u^* \geq u_s(V_{\min})$. The corresponding definition set for z is

$$z \geq z_{\min} = \frac{u_s^2(V_{\min}) - u_s^2(V_m)}{2C_1} = -\frac{\left(V_{\min}^2 - V_m^2\right)^2}{2V_{\min}^2}$$

where the last expression results on using Eqs. (3–5). Consider the denominator of Eq. (23) for $z = z_{\min}$; it shrinks to the expression

$$\frac{V_{\min}^2}{2}\cdot\left[1 - \left(\frac{V_m}{V_{\min}}\right)^4\right] > 0$$

Thus, the limit of F_2 is finite at the lower bound of the defintion set. Together with the monotonicity property (18) of F_2, we obtain the following result about the existence and the uniqueness of u^*: There is a unique solution u^* for $\Delta\chi \leq F_2(u_s(V_{\min}))$.

3) $V_{\min} \leq V_{\max} < V_m$: Now, $u_s(V_{\max})$ is the lower bound for u^*. Again, the limit of F_2 at the lower bound is finite. Just as in the previous case, we conclude: There is a unique solution u^* for $\Delta\chi \leq F_2(u_s(V_{\max}))$.

Remark: The right-hand side of Eq. (23) is not defined for $u^* = u_s(V_m)$, which is equivalent to $z = 0$. Because the limit of F_2 for $z \to 0$ exists, the gap can be closed easily.

B. Two-Phase Extremals

According to the preceding section, three cases are distinguished:

1) $V_{\min} \le V_m \le V_{\max}$: In this case a two-phase extremal does not exist. As stated in Eq. (15), the switching point marks the maximum steady-state turn rate along the trajectory. Because the minimum drag speed V_m, which globally maximizes the u_s value, occurs along the trajectory, V_m would be the only possible switching speed. However, in a sequence $u_+ - u_-$, control switching occurs at the minimum speed passed along the turn. This would imply $V_s = V_m < V_{\min}$ in contradiction to the considered case. An analogous argument excludes the reverse control structure. This negative result corresponds to the existence of single-phase extremals for all commanded turn angles (preceding section).

2) $V_m < V_{\min} \le V_{\max}$: In this case, single-phase trajectories only apply to small turn angles $\Delta\chi$. The following theorem confirms the expectation that the remaining $\Delta\chi$ values are covered by two-phase solutions.

Theorem 4: In the case $V_m < V_{\min} \le V_{\max}$ and $\Delta\chi > F_2(u_s(V_{\min}))$ [F_2 defined in Eq. (23)], the time-optimal turn consists of a $u_+ - u_-$ sequence. The parameter u^* is the unique solution of the equation

$$\Delta\chi = \frac{1}{4C\sqrt{C_1}} \times \ell n\left[\frac{\left(A_1 + z + \sqrt{A_1^2 + B_1 \cdot z}\right) \cdot \left(A_2 + z + \sqrt{A_2^2 + B_2 \cdot z}\right)}{z \cdot \left(z - 2V_m^2\right)}\right] = G_{2b}(u^*) \tag{24}$$

with the abbreviations $A_1 = V_{\max}^2 - V_m^2$, $B_1 = 2V_{\max}^2$, $A_2 = V_{\min}^2 - V_m^2$, $B_2 = 2V_{\min}^2$, z as in Eq. (22), and

$$u^* \in [u_s(V_{\min}),\ u_s(V_m)]$$

Proof: First, we observe that $V_s \ge V_m$. In the case $V_s < V_m$, the minimum drag speed V_m would be passed, and $u^* = u_s(V_s) < u_s(V_m)$ in contradiction to Eq. (15). Therefore, switching occurs under the condition $f_0'(V_s) < 0$. According to Theorem 2, the sequence $u_+ - u_-$ is the only possible structure. Hence, V_s marks the minimum speed along the trajectory, which implies that $V_s < V_{\min}$.

To get G_{2b}, Eq. (16) must be split according to Eq. (19):

$$\Delta\chi = \int_{V_0}^{V_s} \frac{u_+}{\dot V_+}\,\mathrm{d}V + \int_{V_s}^{V_f} \frac{u_-}{\dot V_-}\,\mathrm{d}V = G_{2b}(u^*)$$

Using result (23) for both integrals and the fact that $u^* = u_s(V_s)$ yields Eq. (24). Applying the u_s mapping to the relation $V_m \le V_s < V_{\min}$ obtained earlier yields the definition set for u^*: $u_s(V_{\min}) < u_s(V_s) = u^* \le u_s(V_m)$. In the z domain, the equivalent upper bound is $z \le 0$.

Obviously, G_{2b} is an increasing function of z and, hence, of u^*. G_{2b} tends to infinity for $z \to 0$ and, by directly evaluating G_{2b} and F_2, one confirms that $G_{2b}(u_s(V_{\min})) = F_2(u_s(V_{\min}))$. This determines the value set of G_{2b}; together with the monotonicity, we get the statement of Theorem 4. □

3) $V_{\min} \le V_{\max} < V_m$: Again, single-phase trajectories only occur for small turn angles $\Delta\chi$. All other $\Delta\chi$ values require a two-phase solution:

Theorem 5: In the case $V_{\min} \le V_{\max} < V_m$ and $\Delta\chi > F_2(u_s(V_{\max}))$ [F_2 defined in Eq. (23)], the time-optimal turn consists of a $u_- - u_+$ sequence. The parameter u^* is the unique solution of the equation

$$\Delta\chi = \frac{1}{4C\sqrt{C_1}} \times \ell n\left[\frac{z \cdot \left(z - 2V_m^2\right)}{\left(A_1 + z + \sqrt{A_1^2 + B_1 \cdot z}\right) \cdot \left(A_2 + z + \sqrt{A_2^2 + B_2 \cdot z}\right)}\right] = G_{2c}(u^*) \tag{25}$$

with all symbols declared as in Eq. (24) and

$$u^* \in [u_s(V_{\max}),\ u_s(V_m)]$$

Proof: The proof is very similar to the preceding case 2. Analogous steps lead to $V_{\max} < V_s \le V_m$, implying that $f_0'(V_s) > 0$. According to Theorem 2, there must be a transition from u_- to u_+.

The admissible u^* values are given by $u_s(V_{\max}) < u_s(V_s) = u^* \le u_s(V_m)$, and again $z < 0$. The procedure to get G_{2c} is similar to that given earlier. Again, one can verify $G_{2c}(u_s(V_{\max})) = F_2(u_s(V_{\max}))$ by directly evaluating G_{2c} and F_2. Special difficulties arise on investigating the monotonicity and the limit for $z \to 0 - 0$. (Note that A_1 and A_2 are negative now.) For this purpose, the argument of the ℓn is transformed into

$$\left(1 - \frac{2V_m^2}{z}\right) \cdot \frac{A_1 + z - \sqrt{A_1^2 + B_1 \cdot z}}{2A_1 - B_1 + z} \cdot \frac{A_2 + z - \sqrt{A_2^2 + B_2 \cdot z}}{2A_2 - B_2 + z} \tag{26}$$

Now, the limit ∞ for $z \to 0$ is obvious. Expression (26) is increasing in z for $z < 0$ because each of the three factors has this property. For the first factor, this is obvious. The second and third factors require a somewhat lengthy calculation: For the mapping

$$f(z) = \frac{A + z - \sqrt{A^2 + B \cdot z}}{2A - B + z}$$

the derivative can be written in the form

$$f'(z) = \left(\frac{A - B + \sqrt{A^2 + B \cdot z}}{2A - B + z}\right)^2 \cdot \frac{1}{2\sqrt{A^2 + B \cdot z}} > 0$$

Again, the statement of Theorem 5 is a simple consequence of the results presented earlier. □

Remark 1: In the special case $V_0 = V_f \Leftrightarrow V_{\min} = V_{\max}$, only two-phase solutions occur because $F_2 = 0$.

Remark 2: If u^* is known from Eqs. (24) or (25), the switching speed can be computed from Eqs. (14) and (22):

$$V_s^2 = V_m^2 - z \pm \sqrt{z \cdot \left(z - 2V_m^2\right)} \tag{27}$$

Note that $z < 0$ in the cases 2 and 3. The plus sign belongs to a V_s value greater than V_m. This would be the switching speed for case 2, whereas the minus sign applies in case 3.

VI. Performance as a Feedback Guidance

The optimal feedback control developed in Secs. III–V is used to guide an aircraft with a realistic dynamic model and control constraints. For this purpose, an F-15 model is employed, where T, c_{D0}, and k are functions of the current altitude and Mach number:

$$T = T(h, M), \qquad c_{D0} = c_{D0}(M), \qquad k = k(M) \tag{28}$$

T, c_{D0}, and k are analytic functions adapted to table data of the F-15. The load factor

$$n = \frac{L}{m \cdot g} = \frac{q \cdot S \cdot c_L}{m \cdot g}$$

is bounded by the structural limit

$$n \le n_{\max,1} = 5 \tag{29}$$

and the maximum lift coefficient

$$n \le n_{\max,2} = \frac{q \cdot S \cdot c_{L,\max}(M)}{m \cdot g} \tag{30}$$

where $c_{L,\max}(M)$ again is an analytic model function.

The following algorithm employs the optimal feedback control of the preceding sections as autonomous feedback guidance. It represents a mapping from the current state to the current control.

1) Evaluate T, c_{D0}, and k at the current speed and altitude. With these data, evaluate a_0, a_1, a_2, and C according to Eq. (3a). Set $\Delta\chi$ = desired heading − current heading, V_0 = current speed, V_f = commanded final speed.

2) Use the theorems stated earlier to identify the solution structure (single-phase, two-phase, etc.) associated with the data of step 1.

3) Compute the u^* parameter by numerically solving the corresponding equation. Evaluate u_+ or u_- at $V = V_0$, depending on what type of control is active at the current state. The result is the turn-rate command u.

4) Compute the load factor and the bank angle according to

$$\tan\mu = (V \cdot u)/g, \qquad n = 1/\cos\mu$$

If n exceeds one of the limits (29) or (30), reduce it to $n_1 = \min(n_{\max,1}, n_{\max,2})$ and correct the bank angle according to $\cos\mu = 1/n_1$.

In the sequel, simulation means the numerical integration of the equations of motion

$$\dot{x} = V \cdot \cos\chi, \qquad \dot{y} = V \cdot \sin\chi$$
$$\dot{V} = (T - D)/m, \qquad \dot{\chi} = (g/V) \cdot \tan\mu \tag{31}$$

for flight in the horizontal plane with D according to Eq. (1) and the model functions (28). Each time the integrator calls for the right-hand side of Eqs. (31), the algorithm provides the value of the bank angle. Of course, the output of the algorithm depends on the model version (model 1 or 2) underlying the algorithm. Note that the feedback control 1–4 is not optimal for models (28–30) because the algorithm was designed for constant thrust and drag polar coefficients and unbounded control. What can be expected at best is near optimality in some cases with unbounded or nearly unbounded control.

Three sets of boundary conditions are chosen:

Case A:

$$h = 1500\,\text{m}, \qquad V_0 = 150\,\text{m/s}$$
$$V_f = 300\,\text{m/s}, \qquad \Delta\chi = 180\,\text{deg}$$

Case B:

$$h = 13{,}571\,\text{m}, \qquad V_0 = 500\,\text{m/s}$$
$$V_f = 580\,\text{m/s}, \qquad \Delta\chi = 50\,\text{deg}$$

Case C:

$$h = 13{,}571\,\text{m}, \qquad V_0 = 570\,\text{m/s}$$
$$V_f = 570\,\text{m/s}, \qquad \Delta\chi = 180\,\text{deg}$$

Cases A and B are single-phase turns with $u = u_-$ in the nomenclature of the preceding sections. Case C requires a two-phase solution with the sequence $u_+ - u_-$. Of course, after passing the speed minimum in the simulated trajectory, the internal solution of the four-step algorithm is of single-phase u_- type, too. To check how far in the algorithm generates a time-optimal turn with respect to model (28–30), each simulation is compared to the optimal trajectory for the same boundary conditions. The optimal flight path [optimal with respect to model (28–30)] is computed numerically with a direct multiple shooting approach implemented in the software package GESOP.[4]

A first criterion on the performance of the guidance is the accuracy in the terminal conditions. The simulation stops at the point of which the desired heading is reached. The interesting question is how accurately the speed V_{sim} at this time agrees with the desired value V_f. Another criterion is the flight time t_{sim} in comparison to the minimum time t_{opt} of the optimal trajectory.

Case A: GESOP: $V_f = 300\,\text{m/s}$, $t_{\text{opt}} = 17.11\,\text{s}$
model 1: $V_{\text{sim}} = 303.00\,\text{m/s}$, $t_{\text{sim}} = 17.37\,\text{s}$
model 2: $V_{\text{sim}} = 303.63\,\text{m/s}$, $t_{\text{sim}} = 17.43\,\text{s}$
$190\,\text{kN} \le T \le 235\,\text{kN}$, $0.0193 \le c_{D0} \le 0.0223$,
$0.072 \le k \le 0.079$

Case B: GESOP: $V_f = 580\,\text{m/s}$, $t_{\text{opt}} = 56.35\,\text{s}$
model 1: $V_{\text{sim}} = 579.77\,\text{m/s}$, $t_{\text{sim}} = 56.26\,\text{s}$
model 2: $V_{\text{sim}} = 579.98\,\text{m/s}$, $t_{\text{sim}} = 56.36\,\text{s}$
$115\,\text{kN} \le T \le 135\,\text{kN}$, $0.0433 \le c_{D0} \le 0.0480$,
$0.26 \le k \le 0.37$

Case C: GESOP: $V_f = 570\,\text{m/s}$, $t_{\text{opt}} = 70.45\,\text{s}$
model 1: $V_{\text{sim}} = 569.50\,\text{m/s}$, $t_{\text{sim}} = 73.95\,\text{s}$
model 2: $V_{\text{sim}} = 569.95\,\text{m/s}$, $t_{\text{sim}} = 72.98\,\text{s}$,
$123\,\text{kN} \le T \le 133\,\text{kN}$, $0.0438 \le c_{D0} \le 0.0461$,
$0.303 \le k \le 0.354$

For each simulation with model 2, the range of variation of the quantities T, c_{D0} and k occurring in step 1 is given. It seems that the subsonic case A is not significantly closer to the assumption of constant values T, c_{D0}, and k than the other cases. Although the deviation from the optimal control is small in case A (see Figs. 2 and 3), the simulations miss the terminal value of the speed. The reason is that, at the end of the flight, constraint (29) becomes active, which is not anticipated in the control algorithm. The bank angle reaches its limit $\mu = \arccos(1/n_{\max,1}) = 78.46$ deg (see Fig. 3). This shows that step 4 in the control algorithm is not enough to correct the internal assumption of unbounded control.

Case B is an example with unbounded control; the load factor varies between 1 and 1.4. There is a good agreement of the simulations and the optimal trajectory (see Figs. 4 and 5); the control algorithm really provides a near-optimal control. Model 2 hits the

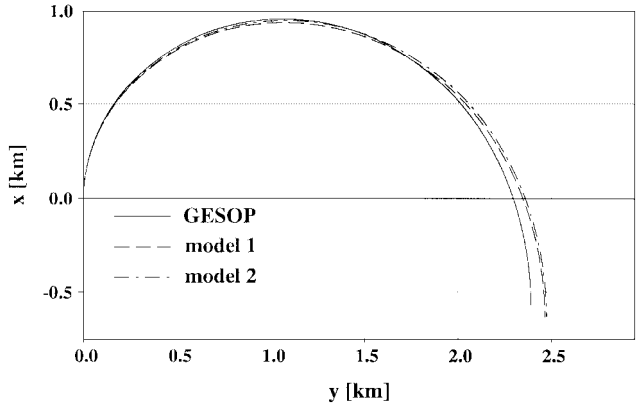

Fig. 2 Case A: ground track.

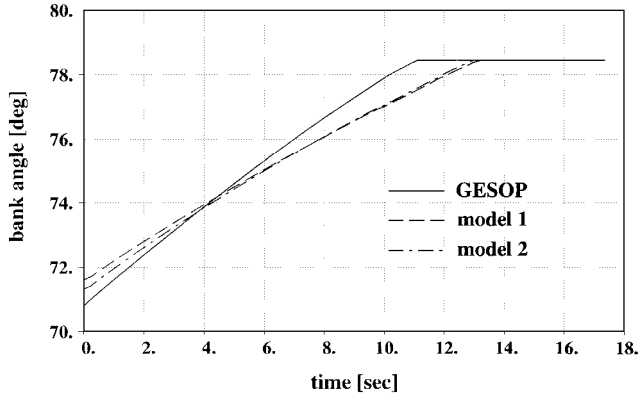

Fig. 3 Case A: bank angle vs time.

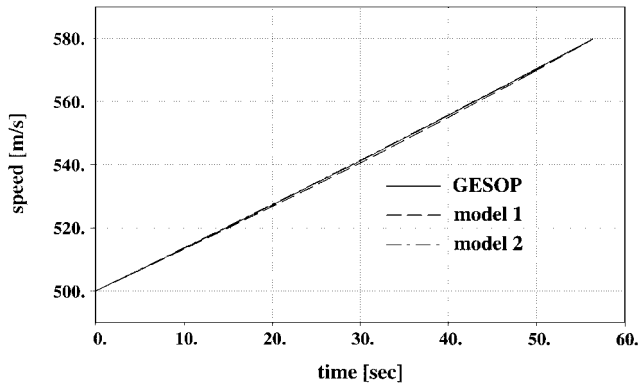

Fig. 4 Case B: velocity vs time.

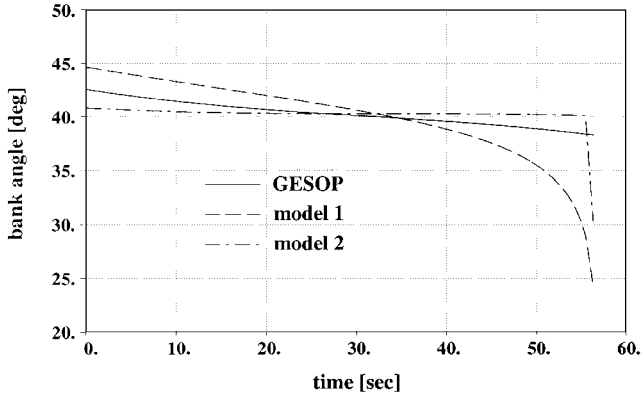

Fig. 5 Case B: bank angle vs time.

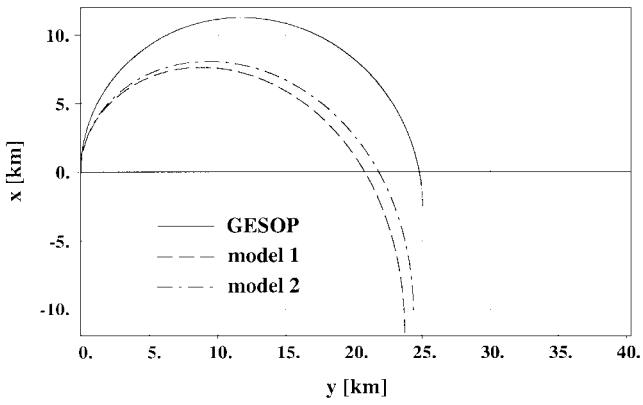

Fig. 6 Case C: ground track.

terminal speed more accurately. The flight time of model 1 is even below the GESOP result; however, there is a miss in the terminal speed of 0.23 m/s.

The control in case C (Figs. 6–9) is unbounded again; only model 1 touches the structural limit (29) near $t = 0$. The simulations reach the terminal speed with satisfactory accuracy, where model 2 is superior again. In both cases B and C, the terminal speed with model 1 is distinctly below the desired value. This may be explained by the fact that a part of the drag is neglected in model 1. The agreement of the simulations and the optimal trajectory is poor in case C. The dotted line in Fig. 7 marks the switching speed V_s according to Eq. (27) with model 2, which is internally computed in the guidance law. Before the speed minimum in the simulation is reached, V_s varies because the input parameters to the control algorithm in step 1 are not constant. The actual speed minimum agrees with the value $V_s = 533$ m/s predicted at this time, and the control algorithm internally switches to a single-phase trajectory with the accelerating control type u_-. The value of V_s is irrelevant thereafter.

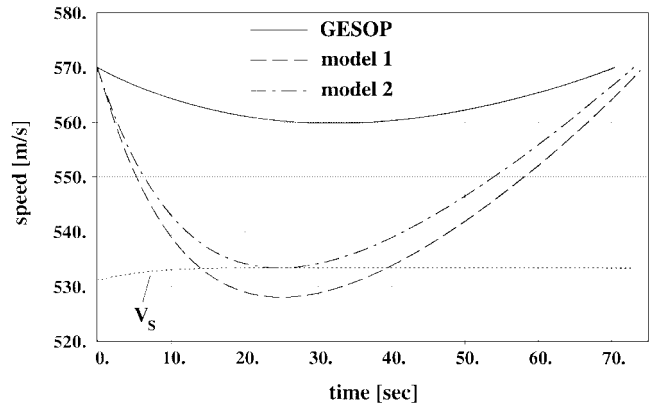

Fig. 7 Case C: velocity vs time (·····, speed minimum predicted by the guidance).

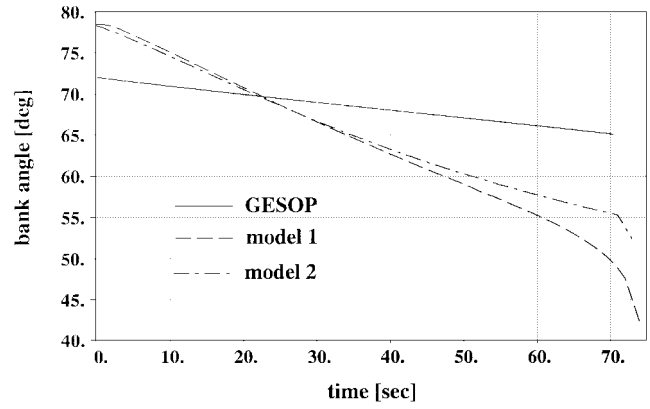

Fig. 8 Case C: bank angle vs time.

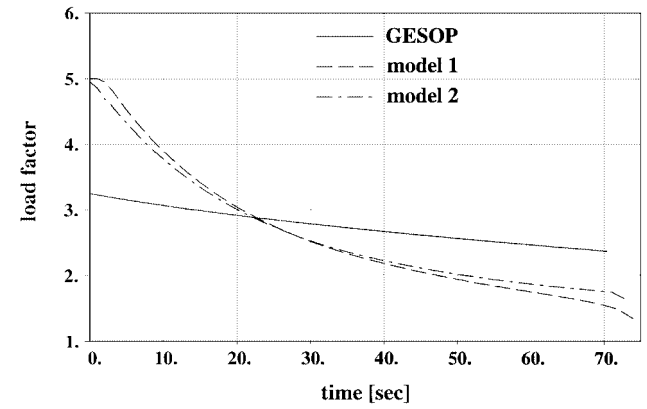

Fig. 9 Case C: load factor vs time.

VII. Conclusions

This paper presents the optimal feedback control in closed form for time-optimal turns in the horizontal plane. At the end of the flight, heading and speed are specified. The main simplifications that are required to obtain analytic solutions are constant thrust and drag polar coefficients and the absence of control constraints. Because of the latter assumption, the results are only valid if the optimal turn rate does not violate a load-factor constraint. Subject to the simplifications presented earlier, two different models are considered. The first one (model 1) neglects the drag induced by the vertical lift component, whereas the second one (model 2) does not. Along the optimal trajectory, two different control types can occur, a decelerating one and an accelerating one. The particular switching structure depends on the initial and final speeds and the commanded heading change. The relation between the switching structure and the boundary conditions is basically different for models 1 and 2.

For both models the switching structure is determined for all boundary conditions within the flight envelope of the aircraft. To evaluate the optimal control as a function of the state, a nonlinear equation must be solved, the form of which depends on the switching structure and the model (1 or 2). In all cases, lower and upper bounds for the unknown parameter are derived and the existence and uniqueness of the solution is proven.

Because of the assumption of an unbounded control, maximum thrust is always optimal. This limits the practical value of the results because partial or minimum thrust can occur along subarcs with maximum load factor. This weakness becomes obvious when the optimal feedback control of model 1 or 2 is used to guide an aircraft with realistic dynamics and control constraints. As long as the bounds on the load factor do not become active, the desired terminal conditions are reached with practically sufficient accuracy, where model 2 is slightly superior. In this case the agreement of the simulated and the optimal flight path (optimal with respect to the realistic aircraft model) depends on the particular boundary conditions.

Another step forward would be to include the load-factor constraints into the design model, which would render the analysis much more complex. Whether the analytic treatment of all possible switching structures succeeds under this extension is an open question.

Acknowledgment

The authors thank Roland Bulirsch for his excellent introduction to optimal control and variational calculus and his advice and support in related applications. This paper is dedicated to this outstanding teacher on the occasion of his 65th birthday.

References

[1]Erzberger, H., and Lee, H. Q., "Optimum Horizontal Guidance Techniques for Aircraft," *Journal of Aircraft*, Vol. 8, No. 2, 1971, pp. 95–101.

[2]Vinh, N. X., *Optimal Trajectories in Atmospheric Flight*, Elsevier, Amsterdam, The Netherlands, 1981, pp. 111–116.

[3]Bulirsch, R., "Die Mehrzielmethode zur numerischen Lösung von nichtlinearen Randwertproblemen und Aufgaben der optimalen Steuerung," Carl-Cranz Gesellschaft Rept., DLR, German Aerospace Research Establishment, Oberpfaffenhofen, Germany, 1971.

[4]Jänsch, C., Schnepper, K., and Well, K. H., "Multiphase Trajectory Optimization Methods with Applications to Hypersonic Vehicles," *Applied Mathematics in Aerospace Science and Engineering*, edited by A. Miele and A. Salvetti, Plenum, New York, 1994, Chap. 8.

[5]Bryson, A. E., Jr., and Ho, Y. C., *Applied Optimal Control: Optimization, Estimation, and Control*, Rev., Hemisphere, New York, 1975, Chap. 6.

[6]Kugelmann, B., and Pesch, H. J., "New General Guidance Method in Constrained Optimal Control, Pt. 1: Numerical Method," and "Pt. 2: Application to Space Shuttle Guidance," *Journal of Optimization Theory and Applications*, Vol. 67, No. 3, 1990, pp. 421–446.

[7]Shinar, J., "Evaluation of Suboptimal Pursuit-Evasion Game Strategies for Air Combat Analysis," AIAA Paper 84-2126, Aug. 1984.

[8]Shinar, J., "Validation of Zero-Order Feedback Strategies for Medium-Range Air-to-Air Interception in a Horizontal Plane," NASA TM 84237, 1982.

[9]Hedrick, J. K., and Bryson, A. E., Jr., "Three-Dimensional, Minimum-Time Turns for a Supersonic Aircraft," *Journal of Aircraft*, Vol. 9, No. 2, 1972, pp. 115–121.

[10]Rajan, N., and Ardema, M. D., "Interception in Three Dimensions—An Energy Formulation," *Journal of Guidance, Control, and Dynamics*, Vol. 8, No. 1, 1985, pp. 23–30.

[11]Ardema, M. D., Rajan, N., and Yang, L., "Three-Dimensional Energy-State Extremals in Feedback Form," *Journal of Guidance, Control, and Dynamics*, Vol. 12, No. 4, 1989, pp. 601–605.

[12]Rajan, N., and Ardema, M. D., "Computation of Optimal Feedback Strategies for Interception in a Horizontal Plane," *Journal of Guidance, Control, and Dynamics*, Vol. 7, No. 5, 1984, pp. 627–629.

[13]Ben-Asher, J. Z., "Optimal Trajectories for an Unmanned Air-Vehicle in the Horizontal Plane," *Journal of Aircraft*, Vol. 32, No. 3, 1994, pp. 677–680.

[14]Clements, J. C., "Minimum-Time Turn Trajectories to Fly-to Points," *Optimal Control, Applications & Methods*, Vol. 11, 1990, pp. 39–50.

[15]Guelman, M., and Shinar, J., "Optimal Guidance Law in the Plane," *Journal of Guidance, Control, and Dynamics*, Vol. 7, No. 4, 1984, pp. 471–476.

[16]Shapira, I., and Ben-Asher, J. Z., "Near-Optimal Horizontal Trajectories for Autonomous Air Vehicles," *Journal of Guidance, Control, and Dynamics*, Vol. 20, No. 4, 1997, pp. 735–741.

[17]Walden, R., "Time-Optimal Turn to a Heading: An Analytic Solution," *Journal of Guidance, Control, and Dynamics*, Vol. 17, No. 4, 1994, pp. 873–875.

[18]Bryson, A. E., Jr., and Ho, Y. C., *Applied Optimal Control: Optimization, Estimation, and Control*, Rev., Hemisphere, New York, 1975, Chap. 2.7.